# Kinetic Analysis of Domino Catalysis: a Case Study on Gold-Catalyzed Arylation

# Kinetic Analysis of Domino Catalysis: a Case Study on Gold-Catalyzed Arylation

Liam T. Ball,[‡†] Tom J. A. Corrie,[‡†] Alexander J. Cresswell,[‡†] and Guy C. Lloyd-Jones*

EaStChem, University of Edinburgh, Joseph Black Building, David Brewster Road, Edinburgh, EH9 3FJ, UK.

*KEYWORDS Domino Catalysis, Kinetics, Catalyst Speciation, Mechanism, Sequence-Selectivity*

**ABSTRACT:** Domino catalysis is a well-explored route to increasing the efficiency of multistep reactions. However, the kinetic features required for efficient turnover of a process where "multiple transformations are effected by a single catalytic mechanism" have not been explored in any detail. The kinetics of a nominally simple two-stage domino catalytic reaction have been analyzed by way of a gold-catalyzed coupling of two electron-deficient arylsilanes to generate an arylated fluorene. A combination of in situ interleaved $^{1}$H and $^{19}$F NMR spectroscopic kinetic measurements, kinetic simulations, and variations in substitution, reveal how the catalyst partitioning between the two different cycles impacts on both the rate and selectivity of the process. The insight enables identification that sequential catalyst speciation and accumulation of the domino intermediate are general kinetic criteria for efficient domino catalysis.

## Introduction

Efficiency and selectivity lie at the heart of modern synthetic chemistry.[1-3] In this context, 'domino'[4,5] and 'tandem'[5,6] catalyses, in which two or more discrete bond-forming steps take place under the same conditions, provide valuable increases in the net efficiency per unit-operation.[3] Fogg and dos Santos distinguish domino processes, Scheme 1, as those adhering to Tietze's original definition[4] but where "*multiple transformations are effected by a single catalytic mechanism*".[5] Conversely, tandem catalysis denotes "coupled catalyses in which sequential transformation of the substrate occurs *via* two (or more) mechanistically-distinct processes".[5]

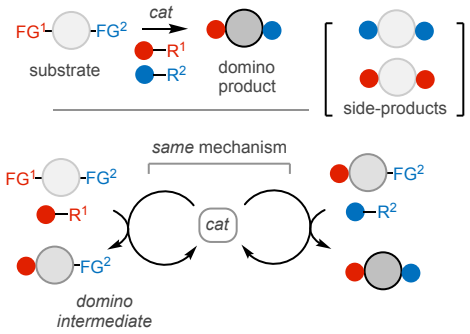


**Scheme 1**. A generic two-stage domino catalytic process. FG = functional group, R = reagent.

As illustrated below, this specific requirement for the domino process can have profound kinetic implications. However, as far as we are aware, the kinetics of domino catalysis have not been explored in any detail.[6k] Herein, we report on an in situ $^{1}$H/$^{19}$F NMR spectroscopic and kinetic study of a two-stage domino process, deconvolution of which provides general insight to the requirements for efficient catalysis.[4,5]

## Discussion

A variety of C–H functionalizations have been developed into domino transformations,[7-9] including direct-arylations,[10,11] and we selected a gold-catalyzed process[12-18] (**1** + **2**; Scheme 2) for kinetic studies. Whilst conceptually simple, it requires a selective 'intra-inter'[19] sequence, within an array of C–H bonds.

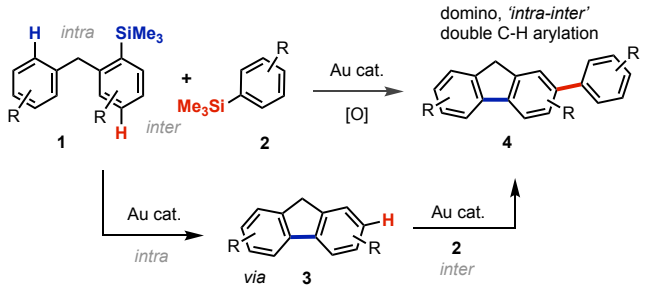


**Scheme 2**. Domino C–H arylation of arylsilane **1** with arylsilane **2** to generate arylated-fluorene **4**, *via* **3**.

The mechanism for both stages in the domino-sequence involves C–Si auration of the silane,[20] followed by C–H auration of the arene, via $S_E$Ar-type reactions of Ar-[Au$^{III}$] intermediates,[21] Scheme 3. The regio- and chemo-selectivities are consistent with previous observations, including the sterically-enhanced reactivity of ortho-substituted aryl-silanes (**1**) towards auration,[12c] and the regioselective arylation of fluorenes (**3**).[13]

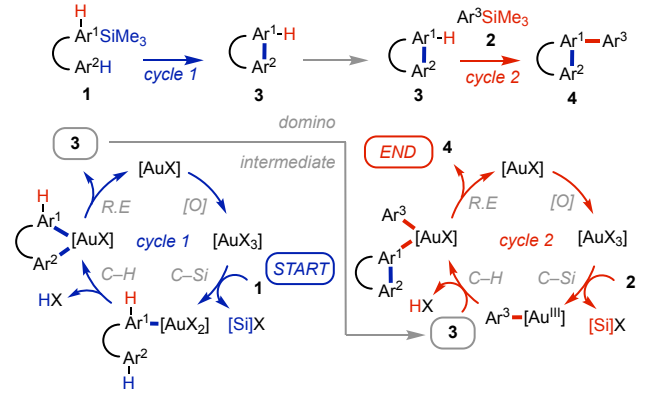


**Scheme 3**. Domino-catalyzed arylation, highlighting that both cycles proceed via the same overarching mechanism.

**1. Preliminary Kinetic Analysis and Impact of Sequence Selectivity ($k_1/k_2$).** To gain an understanding of how the two

separate, but linked, catalytic cycles (1 and 2, Scheme 3) dictate the kinetics of the overall domino process, we began by analysing the kinetics of domino cycle one, and domino cycle two *in isolation*.[22] We then combined the two sets of data in kinetic simulations. Cyclisation of **1a** gave chlorofluorene **3a**;[15a] this was then reacted with *p*-F-**2**, to give *p*-F-**4a**, Scheme 4. Rate-coefficients for the turnover-rate limiting steps in the two processes, intramolecular reductive-elimination of **3a** ($k_{intra}$),[15a] and intermolecular reaction with fluorenes **3a** and **4a** ($k_{inter}$, and $k_{over}$),[13] were then extracted by simulation (see SI).

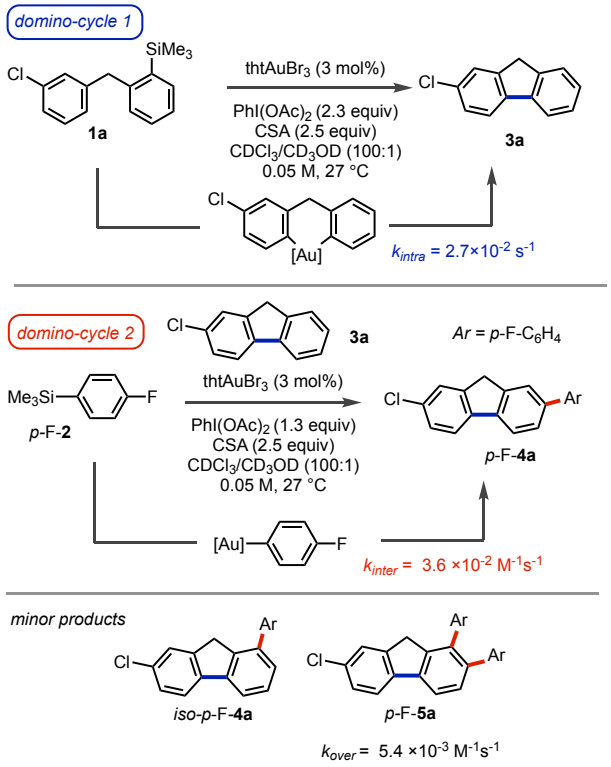


**Scheme 4**. Independently determined rate coefficients for turnover-rate limiting processes[13,15] in *isolated* domino-cycles. CSA = camphorsulfonic acid; tht = tetrahydrothiophene.

With kinetic data available for some of the individual steps, Scheme 4, the domino process in which **1a** + *p*-F-**2** react to generate **3a** and then *p*-F-**4a**, Figure 1, was explored by simulation. Using the model, we extensively probed the effect of the partitioning[23] of the catalyst across the two domino cycles ($k_1$ and $k_2$). *This revealed two phenomenologically distinct zones, separated by a threshold value of* $k_1/k_2 = 1$. When there is high selectivity for cycle 1 over cycle 2 ($k_1/k_2 >> 1$), the domino intermediate (**3a**) accumulates substantially, and then decays as it undergoes consumption by cycle 2 (Scheme 3), Figure 1A. The rate of generation of the final domino product does not change significantly when $k_1/k_2 \geq 10$ (see SI).

As the selectivity is reduced and $k_1/k_2$ approaches and reaches 1:1 (i.e. no selectivity for cycle 1 over cycle 2), a low steady-state concentration of the domino intermediate (**3a**) is generated, leading to a much slower evolution of the final domino product *p*-F-**4a**, Figure 1B. Under these conditions, the domino intermediate (**3a**) does not accumulate because it is generated in equimolar flux ($k_1/k_2 = 1$; $[\mathbf{1a}]_0 = [\mathbf{2a}]_0$) with the catalytic intermediate by which it is then captured ($k_{inter}$).

As the ratio $k_1/k_2$ is reduced below unity, *there is a profound change in the evolution of the model catalytic system.* Each formal revolution of the cycle produces a deficiency of the domino intermediate with which the cycle 2 catalyst intermediate (Ar-Au) must react ($k_{inter}$) to release catalyst required for cycle 1 (see 'start' in Scheme 3). As a consequence, with every turnover, the catalyst is further sequestered in an increasing reservoir on cycle 2, and, *for a highly chemoselective process in which* $k_1/k_2 < 1$, *catalysis will stall,* Figure 1C, at a point dictated by the initial catalyst loading.

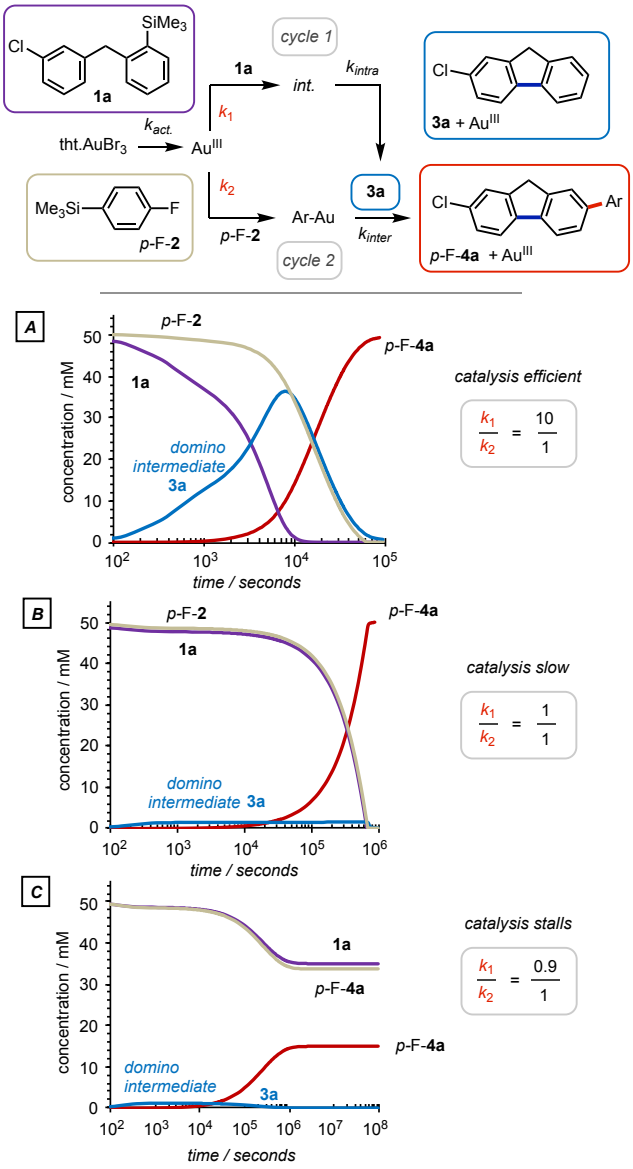


**Figure 1.** The impact of the C–Si partition ($k_1/k_2$) on the efficiency of an *exclusively* 'intra-inter'[11] domino sequence where $[\mathbf{1a}]_0 = [p\text{-F-}\mathbf{2}]_0 = 0.05$M; 3 mol% Au(III); $k_{act} = 7 \times 10^{-3}$ s$^{-1}$; $k_{intra} = 2.7 \times 10^{-2}$ s$^{-1}$; $k_{inter} = 3.6 \times 10^{-2}$ M$^{-1}$s$^{-1}$; and there is no homocoupling[12,13] or over-arylation ($k_{over}$). See SI for a larger series of plots, where the $k_1/k_2$ partition ranges from 0.5 to 100.

**2. Experimental Domino Catalysis data for 1a + *p*-F-2 and Kinetic Simulation.** With insight into the impact of the cycle partitioning ($k_1/k_2$) Figure 1, the full experimental kinetic profile for the domino process was determined, Figure 2. Interleaved in situ $^1$H and $^{19}$F NMR spectroscopic analysis of the reaction of **1a** with *p*-F-**2** revealed a significant accumulation of fluorene

**3a** in the early stages of reaction, followed by decay in **3a** to give the domino arylation product *p*-F-**4a**, plus minor side-products *p*-F-*iso*-**4a** and *p*-F-**5a**. The kinetic model constructed from the experimentally-estimated reference rate coefficients (Scheme 3) proved capable of simulating the temporal concentration data with reasonable accuracy when the C–Si auration partition was set to $k_1/k_2$ = 25:1, Figure 2. The high $k_1/k_2$ ratio (~25) is consistent with the general effect of *ortho*-substituents accelerating C–Si auration by one to two orders of magnitude; a phenomenon attributed to alleviation of ground-state steric strain on approach to a pseudo-tetrahedral transition-state.[12c,13]

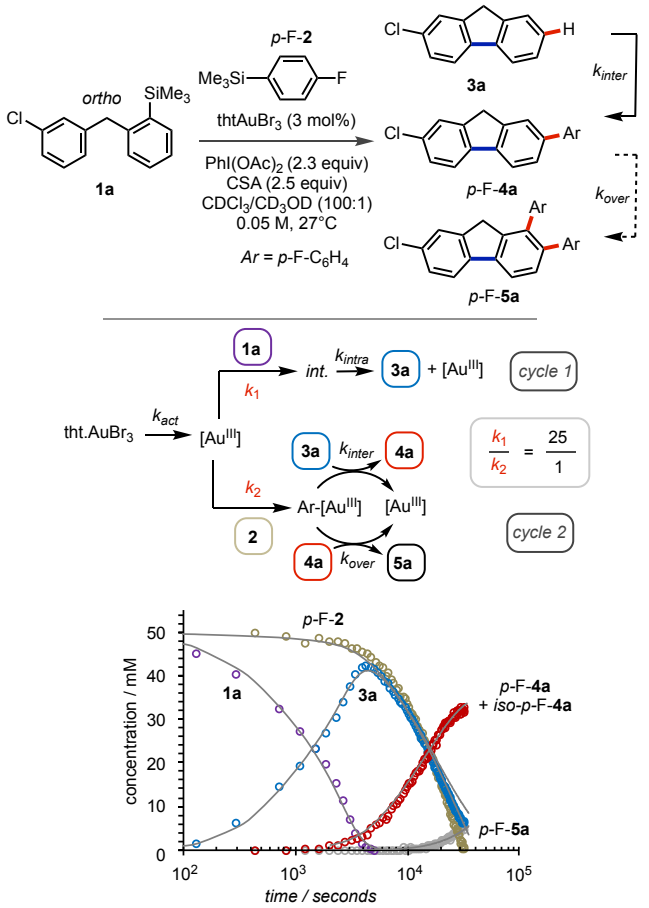


**Figure 2.** Domino reaction of **1a** with *p*-F-**2**, analysed by in situ $^1$H and $^{19}$F NMR spectroscopy against an internal standard. Lower section, kinetic simulation (solid lines) using model shown with: $k_{act} = 7 \times 10^{-3}$ s$^{-1}$; $k_{intra} = 2.5 \times 10^{-2}$ s$^{-1}$; $k_{inter} = 3.9 \times 10^{-2}$ M$^{-1}$s$^{-1}$; $k_{over} = 5.4 \times 10^{-3}$ M$^{-1}$s, and $k_1/k_2$ = 25/1. Products *p*-F-**4a** and *iso*-*p*-F-**4a**, generated in 88:12 *rr*, are treated as a single component in the model. For details see SI.

**3. Perturbation of the Domino Sequence-Selectivity ($k_1/k_2$).** The effect of perturbation of the reactivity of both coupling partners in the domino sequence, by electron-withdrawing groups (X, Z), was explored next. To simplify the analysis, 2,4-dimethylated arysilanes (**1b-e**, Table 1) were employed. The additional methyl groups on the ortho-benzyl group have the effect of limiting the C–H auration steps to the more electron-rich ring; the increased steric hindrance also suppresses over-arylation (→**5**) of the primary products. Domino arylation proceeded with regioselectivity ranging from 60/40 to >99/1, Table 1. Isolated fluorene intermediates **3** were found to undergo Au-catalyzed arylation by **2** with significantly higher regioselectivity than those obtained by the domino reactions,[24] thus the **4**/*iso*-**4** ratios in Table 1 primarily reflect the change in $k_1/k_2$, see Figure 3.

**Table 1.** Effect of electron-withdrawing groups (X,Z) substituents *para* to the silane,[25] on the partitioning ($k_1/k_2$) and selectivity (**4**/*iso*-**4**) in the domino reaction of **1** with **2**; conditions as Figure 2.

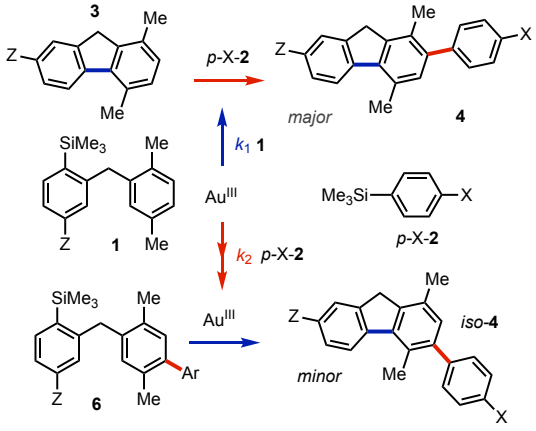


| entry | X | Z | *product* | yield / %[a] | **4** / *iso*-**4** |
|---|---|---|---|---|---|
| 1 | F | H | *p*-F-**4b** | 46 | 96:44[b] |
| 2 | F | F | *p*-F-**4c** | 67 | 95:5 |
| 3 | F | Cl | *p*-F-**4d** | 50 | 93:7 |
| 4 | F | $CF_3$ | *p*-F-**4e** | 77[c,d] | 60:40 |
| 5 | H | F | *p*-H-**4c** | 64 | 94:6 |
| 6 | Br | F | *p*-Br-**4c** | 71 | 94:6 |
| 7 | $CF_3$ | F | *p*-$CF_3$-**4c** | 78 | >99:1 |

[a.] With the exception of *p*-F-**4e**, yields are for isolated purified products in the *rr* stated.[23] [b.] 17% of the diarylated product was also isolated. [c.] Reaction was run at 50 °C. [d.] Yield estimated by $^{19}$F NMR spectroscopy using an internal standard.

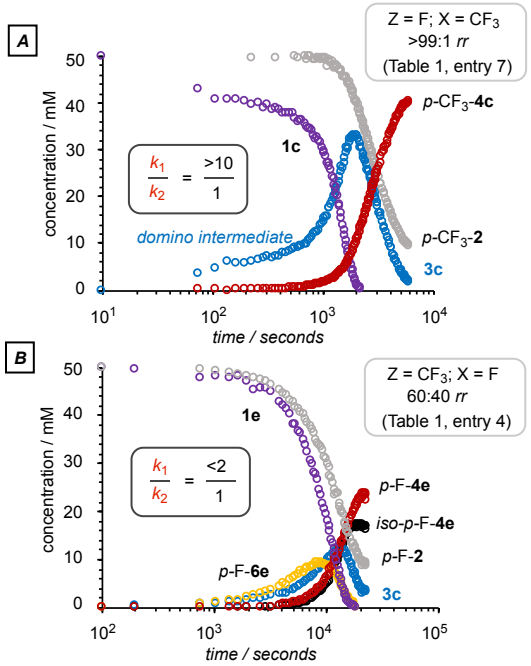


**Figure 3.** Graph A: selective accumulation of intermediate **3c**, indicative of high 'intra-inter' selectivity. Graph B, low 'intra-

inter' selectivity, with accumulation of intermediates **3c** and p-F-**6e**. Reactions analysed in situ by $^{19}$F NMR spectroscopy.[26]

Comparison of the in situ $^{19}$F NMR spectroscopic analysis (Figure 3) of the domino reactions in Table 1 entries 4 and 7, illustrates the impact of modulation of $k_1/k_2$. Increased electron-demand in the *intermolecular* arylating agent, **2** attenuates $k_2$,[25] thus raising $k_1/k_2$ and affording high efficiency and selectivity, see Figure 3A. Conversely, increased electron-demand in the *intramolecular* arylation substrate, **1e**, attenuates $k_1$,[25] thus reducing $k_1/k_2$ and leading to lower efficiency and selectivity; see Figure 3B. The *selective* accumulation of the domino intermediate (fluorene **3c**; Figure 3A) is characteristic of a high $k_1/k_2$ ratio: neither of the isomeric products (**6** or *iso*-*p*-F-**4c**) are detected. In contrast, for the reaction of the electron-deficient arylsilane **1e**, Figure 3B, where the $k_1/k_2$ ratio is closer to unity, intermediates on *both* pathways (**3e** and *p*-F-**6**) are detected.[26] Whilst the impact of electron-donating groups, such as Me and MeO, on the silyl-bearing aryl rings in **1** and **2**, was not explored in this kinetics-focussed study, it is anticipated that silane-homocoupling will begin to dominate over cross-coupling for both the intermolecular[12a,13] and intramolecular[15] pathways. The use of analogous substrate pairs based on Schoenbeck's $ArGeEt_3$ reagents[16] may provide a solution to this issue.

**4. General Kinetic Prerequisites for Domino Catalysis.** From the studies described above, and applying the definition of Fogg and dos Santos,[5] a number of general kinetic prerequisites can be identified for the successful concatenation of reactions via "a single catalytic mechanism".[4-6] As discussed below, whilst it is obvious that *selectivity* is required, there are subtleties to this selectivity that are not intuitive, and warrant careful consideration in new domino sequences.

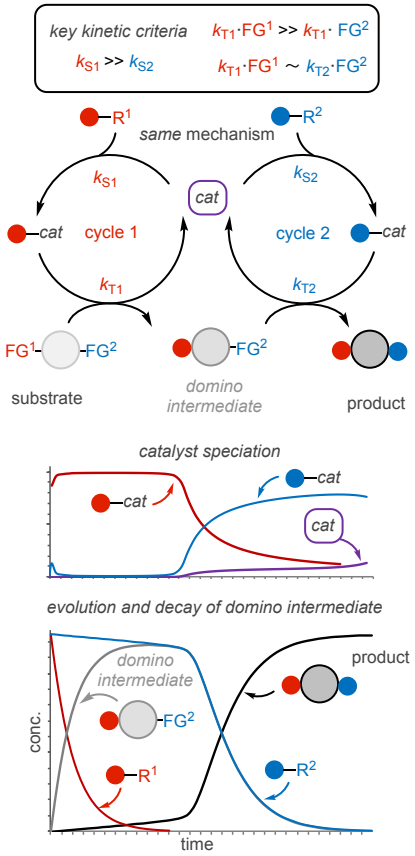


**Scheme 5.** Generic two-cycle domino catalysis, and kinetic criteria for efficiency, together with temporal catalyst speciation and evolution of intermediates and products. ($k_{S1}$ = 100 $k_{S2}$; $k_{T1}$.FG$^1$ = $k_{T2}$.FG$^2$; $k_{T1}$.FG$^2$ = $k_{T2}$.FG$^1$ = 0). See text for full discussion.

To simplify the discussion, we refer to four steps ($k_{S1}$, $k_{T1}$, $k_{S2}$, $k_{T2}$) in the generic domino sequence in Scheme 5. The process involves reaction of a substrate bearing two functional groups (FG$^1$ and FG$^2$) with two reagents (R$^1$ and R$^2$) via a domino-intermediate. We use rate coefficients ($k$) as shorthand for rates, noting that for this and alternative domino processes, individual steps can be intra- or inter-molecular, and thus rate-ratios can vary as the reactions evolve and reactant concentrations change.

Avoiding cross-reactivity (R$^1$ + FG$^2$, and R$^2$ + FG$^1$) is essential to avoid side-products. However, the complementary pairs of the functional groups reacting in each of the two stages of the desired sequence (i.e. R$^1$ + FG$^1$, and then R$^2$ + FG$^2$) must, by definition,[5] be similar and possibly even identical: *they have to react via the same catalytic mechanism*. Thus, compared to a normal (non-domino) process, there needs to be additional control-factor(s) that allow selective, chronologically-distinct, coupling of two (or more) pairs of functional groups by a *single* mechanism.

A primary component of such control, is that there is a succession in catalyst speciation between the two (or more) stages of the domino sequence, Scheme 5. The catalyst must enter cycle 1 ($k_{S1}$) in preference to cycle 2 ($k_{S2}$), until the reagents for the first stage of the domino reaction are consumed. The catalyst intermediate (R$^1$-cat) on cycle 1, must also react selectively with FG$^1$ over FG$^2$, so that the domino intermediate is generated, rather than producing a side-product, or worse, generating an inhibited catalyst. (see Figure 1C). This combination of two selectivity factors ensures maximum accumulation of the domino intermediate (see e.g. Figure 2) before significant engagement of the next stage in catalysis. However, if this selectivity is achieved by cycle 2 reactions ($k_{S2}$, $k_{T2}$) that are *inherently* slow, then the overall domino process will be inefficient, not due to undesired side-reactions, but due to slow turnover in the second stage: in essence one loses the advantages of conducting the process as a domino sequence.

## Conclusions

We have reported the first kinetic studies on domino catalysis, employing a sequential coupling of two arylsilanes (**1** and **2**), as a vehicle to explore the factors that control rate, selectivity, and ultimately the feasibility of the process. Beginning by analysis of the kinetics of isolated (non-domino) intermolecular[12-14] and intramolecular[15] arylations, we were able to develop a quantitative analysis of the kinetics of the corresponding domino process (Figures 1 and 2), and interpret the contrasting effects on the selectivity induced by substituents on the two aryl silanes (**1**, **2**; Figure 3). Elucidation of the features that allow effective coupling of **1** and **2**, albeit presently limited to the testing of substrates containing electron-donating groups on the silyl-bearing aryl rings, lead to a more-general consideration of selectivity in the context of domino catalysis: reactions proceeding via "a single catalytic mechanism".[4-6]

Overall it can be concluded that efficient (selective *and* fast) domino catalyses must employ *two different* strategies to meet two kinetic prerequisites. Firstly, steps that partition reagents into the catalytic cycle, should ideally be fast relative to other steps: in such a way, the succession of catalyst speciation (i.e.

into cycle 1, then cycle 2 and so on) can be attained by inherent rate differentials, e.g. $k_{S1}>>k_{S2}$, Scheme 5, without compromising the overall rate of the domino process. Secondly, the step that involves the reaction of the domino intermediate should be biased in some way, e.g. by molecularity, or by modulation of the inherent reactivity of the functional group ($FG^2$ in Scheme 5). To illustrate the latter, consider the domino intermediate (fluorene **3**) in Figure 3A. The conjugated rings in the domino intermediate make it considerably more reactive to arylation by Ar-Au than either of the two aromatic rings in **1**. However, accumulation of this domino intermediate is assured by i) faster reaction of the ortho-substituted silane **1** ($k_1>>k_2$; due to steric effects) and ii) rapid *intramolecular* C–H functionalization. The *combination of both features* secures the requisite overall selectivity.

In general, the hallmark of efficient domino catalysis is the accumulation[27] of the domino intermediate whilst turnover of cycle 1 dominates, followed by efficient consumption of the domino intermediate by cycle 2, see e.g. Figure 2 and Scheme 5. Conditions under which either of the two selectivity criteria highlighted above are only marginally satisfied, will lead to competing processes, or to complete catalyst inhibition.[28] The criteria elucidated impact on the rate, selectivity, and ultimately feasibility of the catalytic process, and can be used to augment general guiding principles in the design of substrates and conditions for 'domino',[4] and 'auto-tandem' catalytic reactions.[4-6]

## AUTHOR INFORMATION


### Corresponding Author

* guy.lloyd-jones@ed.ac.uk

### Present Addresses

† L.T.B: School of Chemistry, University Park, Nottingham, NG7 2RD, U.K.
T.J.A.C: Syngenta, Jealott's Hill International Research Centre, Berkshire, RG42 6EY, U.K.
A. J. C: School of Chemistry, University of Bath, Bath, BA2 7AY, U.K.

### Author Contributions

‡These authors contributed equally.



### Funding Sources

The research leading to these results has received funding from the European Research Council under the European Union's Seventh Framework Programme (FP7/2007-2013) / ERC grant agreement n° [340163].


## ASSOCIATED CONTENT

**Supporting Information**. Experimental procedures, simulation, substrate and product characterization data and NMR spectra. This material is available free of charge via the Internet at http://pubs.acs.org.

## ACKNOWLEDGMENT


We thank the University of Edinburgh for support.


## REFERENCES


(1) Trost, B. M. Atom Economy—A Challenge for Organic Synthesis: Homogeneous Catalysis Leads the Way. *Angew. Chem. Int. Ed. Engl.* **1995**, *34*, 259–281.

(2) Wender, P. A.; Verma, V. A.; Paxton, T. J.; Pillow, T. H. Function-Oriented Synthesis, Step Economy, and Drug Design. *Acc. Chem. Res.* **2008**, *41*, 40–49.

(3) Hayashi, Y. Pot economy and one-pot synthesis. *Chem. Sci.* **2016**, *7*, 866–880.

(4) Tietze defined 'domino' reactions as those involving "two or more bond-forming transformations which take place under the same reaction conditions, without adding additional reagents or catalysts, and in which the subsequent reactions result as a consequence of the functionality formed in the previous step". See: Tietze, L. F. Domino Reactions in Organic Synthesis. *Chem. Rev.* **1996**, *96*, 115–136.

(5) Fogg D. E.; dos Santos, E. N. Tandem catalysis: a taxonomy and illustrative review. *Coord. Chem. Rev.* **2004**, *248*, 2365–2379.

(6) For selected reviews on domino/tandem reactions, see: a) *Applications of Domino Transformations in Organic Synthesis* (Ed. S. A. Synder), Science of Synthesis; Thieme: Stuttgart, **2016**; Volume 1, pages 449–632; b) Zielinski, G. K.; Grela, K. Tandem Catalysis Utilizing Olefin Metathesis Reactions. *Chem. Eur. J.* **2016**, *22*, 9440 – 9454. c) Lohr T. L.; Marks, T. J. Orthogonal tandem catalysis. *Nature Chem.* **2015**, *7*, 477–482; d) *Domino Reactions* (Ed. L. F. Tietze), Wiley-VCH, Weinheim, **2014**; e) Zhou, J. Recent Advances in Multicatalyst Promoted Asymmetric Tandem Reactions. *Chem. Asian J.* **2010**, *5*, 422–434; f) Shindoh, N.; Takemoto, Y.; Takasu, K. Auto-Tandem Catalysis: A Single Catalyst Activating Mechanistically Distinct Reactions in a Single Reactor. *Chem. Eur. J.* **2009**, *15*, 12168–12179; g) Chapman C. J.; Frost, C. G. Tandem and Domino Catalytic Strategies for Enantioselective Synthesis. *Synthesis* **2007**, 1–21; h). Nicolaou, K. C.; Edmonds D. J.; Bulger, P. G. Cascade Reactions in Total Synthesis. *Angew. Chem. Int. Ed.* **2006**, *45*, 7134–7186; i) Wasilke, J.-C.; Obrey, S. J.; Baker R T.; Bazan., G. C. Concurrent Tandem Catalysis. *Chem. Rev.* **2005**, *105*, 1001–1020; j) Nicolaou, K. C.; Montagnon T.; Synder, S. A. Tandem reactions, cascade sequences, and biomimetic strategies in total synthesis. *Chem. Commun.* **2003**, 551–564; k) Mayer, S. F.; Kroutil W.; Faber, K. Enzyme-initiated domino (cascade) reactions. *Chem. Soc. Rev.* **2001**, 332–339; l) Ikeda, S. Nickel-Catalyzed Intermolecular Domino Reactions. *Acc. Chem. Res.* **2000**, *33*, 511–519; m) Poli, G.;. Giambastiani G.; Heumann, A. Palladium in Organic Synthesis: Fundamental Transformations and Domino Processes. *Tetrahedron* **2000**, *56*, 5959–5989; n) de Meijere A.; Brase, S. Palladium in action: domino coupling and allylic substitution reactions for the efficient construction of complex organic molecules. *J. Organomet. Chem.* **1999**, *576*, 88–110; o) Malacria, M. Selective Preparation of Complex Polycyclic Molecules from Acyclic Precursors via Radical Mediated- or Transition Metal-Catalyzed Cascade Reactions. *Chem. Rev.* **1996**, *96*, 289–306; p) Padwa A.; Weingarten, M. D. Cascade Processes of Metallo Carbenoids. *Chem. Rev.* **1996**, *96*, 223–270; q) Wang, K. K. Cascade Radical Cyclizations via Biradicals Generated from Enediynes, Enyne-Allenes, and Enyne-Ketenes. *Chem. Rev.* **1996**, *96*, 207–222; r) Parsons, P. J.; Penkett, C. S.; Shell, A. J. Tandem Reactions in Organic Synthesis: Novel Strategies for Natural Product Elaboration and the Development of New Synthetic Methodology. *Chem. Rev.* 1996, **96**, 195–206; s) Denmark, S. E.; Thorarensen, A. Tandem [4+2]/[3+2] Cycloadditions of Nitroalkenes. *Chem. Rev.* **1996**, *96*, 137–166; t) Heumann A.; Reglier, M. The stereochemistry of palladium catalysed cyclisation reactions part C: Cascade reactions. *Tetrahedron* **1996**, *52*, 9289–9346; u) Tietze L. F.; Beifuss, U. Sequential Transformations in Organic Chemistry: A Synthetic Strategy with a Future. *Angew. Chem. Int. Ed. Engl.* **1993**, *32*, 131–163; v) Ho, T.-L. *Tandem Organic Reactions*, Wiley, New York, **1992**; w) Hoffmann, H. M. R. Cascade Cyclizations. *Angew. Chem. Int. Ed. Engl.* **1992**, *31*, 1332–1334.

(7) For an intermolecular Heck, intramolecular C–H arylation sequence using palladium catalysis, see: Leclerc, J.-P.; André M.; Fagnou, K. Heck, Direct Arylation, and Hydrogenation: Two or Three Sequential Reactions from a Single Catalyst. *J. Org. Chem.* **2006**, ***71***, 1711–1714.

(8) See for example, Pitts, A. K.; O'Hara, F.; Snell R. H.; Gaunt, M. J. A Concise and Scalable Strategy for the Total Synthesis of Dictyodendrin B Based on Sequential C–H Functionalization. *Angew. Chem. Int. Ed.* **2015**, *54*, 5451–5455.

(9) For selected recent examples see: a) Sickert, M.; Weinstabl, H.; Peters, B.; Hou, X.; Lautens, M. Intermolecular Domino Reaction of Two Aryl Iodides Involving Two C□H Functionalizations. *Angew. Chem. Int. Ed.* **2014**, *53*, 5147–5151; b) Huang, R. Y.; Franke, P. T.; Nicolaus, N.; Lautens, M. Domino C–H functionalization reactions of gem-dibromoolefins: synthesis of N-fused benzo[c]carbazoles. *Tetrahedron* **2013**, *69*, 4395–4402; c) Liu, H.; El-Salfiti M.; Lautens, M. Expeditious Synthesis of Tetrasubstituted Helical Alkenes by a Cascade of Palladium-Catalyzed C–H Activations. *Angew. Chem. Int. Ed.* **2012**, ***51***, 9846–9850.

(10) For reviews on direct-arylation, see: a) Dey A.; Maity S.; Maiti D. Reaching the south: metal-catalyzed transformation of the aromatic para-position. *Chem. Commun*. **2016**, *52*, 12398-12414; b) Liu, C.; Yuan, J.; Gao, M.; Tang, S.; Li, W.; Shi, R.; Lei, A. Oxidative Coupling between Two Hydrocarbons: an Update of Recent C–H Functionalizations. *Chem. Rev.* **2015**, *115*, 12138–12204; c) Yamaguchi, J.; Yamaguchi, A. D.; Itami, K. C–H Bond Functionalization: Emerging Synthetic Tools for Natural Products and Pharmaceuticals. *Angew. Chem. Int. Ed.* **2012**, *51*, 8960–9009; d) Ackermann, L. Carboxylate-Assisted Transition-Metal-Catalyzed C−H Bond Functionalizations: Mechanism and Scope. *Chem. Rev.* **2011**, *111*, 1315–1345; e) Lyons, T. W.; Sanford, M. S. Palladium-Catalyzed Ligand-Directed C−H Functionalization Reactions. *Chem. Rev.* **2010**, *110*, 1147–1169; f) Ackerman, L.; Vicente, R.; Kapdi, A. R. Transition-Metal-Catalyzed Direct Arylation of (Hetero)Arenes by C–H Bond Cleavage. *Angew. Chem. Int. Ed.* **2009**, *48*, 9792–9826; g) McGlacken, G. P.; Bateman, L. M. Recent Advances In Aryl–Aryl Bond Formation By Direct Arylation. *Chem. Soc. Rev.* **2009**, *38*, 2447–2464.

(11) see e.g. a) Saget, T.; Perez D.; Cramer, N. Synthesis of Functionalized Spiroindolines via Palladium-Catalyzed Methine C–H Arylation. *Org. Lett.* **2013**, *15*, 1354–1357. b) Ghosh, K.; Rit, R. K.; Ramesh, E.; Sahoo, A. K. Ruthenium-Catalyzed Hydroarylation and One-Pot Twofold Unsymmetrical C–H Functionalization of Arenes Angew. *Chem. Int. Ed*. **2016**, *55*, 7821 –7825.

(12) Intermolecular Au-catalyzed arylation of arenes by aryl silanes: a) Ball, L. T.; Lloyd-Jones, G. C.; Russell, C. A. Gold-Catalyzed Direct Arylation. *Science* **2012**, *337*, 1644–1648; b) Hua, Y.; Asgari, P.; Avullala, T.; Jeon, J. Catalytic Reductive ortho-C−H Silylation of Phenols with Traceless, Versatile Acetal Directing Groups and Synthetic Applications of Dioxasilines. *J. Am. Chem. Soc.* **2016**, *138*, 7982–7991; c) Robinson M. P.; Lloyd-Jones, G. C. Au-Catalyzed Oxidative Arylation: Chelation-Induced Turnover of ortho-Substituted Arylsilanes. *ACS Catalysis* **2018**, **8**, 7484–7488.

(13) Ball, L. T.; Russell, C. A.; Lloyd-Jones, G. C. Gold-Catalyzed Oxidative Coupling of Arylsilanes and Arenes: Origin of Selectivity and Improved Precatalyst. *J. Am. Chem. Soc.* **2014**, *136*, 254–264.

(14) Intermolecular Au-catalyzed arylation of heteroarenes by aryl silanes: a) Cresswell, A. J.; Lloyd-Jones, G. C. Room-Temperature Gold-Catalysed Arylation of Heteroarenes: Complementarity to Palladium Catalysis. *Chem. Eur. J.* **2016**, *22*, 12641–12645; b) Hata, K.; Ito, H.; Segawa, Y.; Itami, K. Pyridylidene Ligand Facilitates Gold-Catalyzed Oxidative C–H Arylation of Heterocycles. *Beilstein J. Org. Chem.* **2015**, *11*, 2737–2746;

(15) Intramolecular Au-catalyzed arylation of arenes by aryl silanes: a) Corrie, T. J. A.; Ball, L. T.; Russell, C. A.; Lloyd-Jones, G. C. Au-Catalyzed Biaryl Coupling To Generate 5- to 9-Membered Rings: Turnover-Limiting Reductive Elimination versus π-Complexation. *J. Am. Chem. Soc.* **2017**, *139*, 245–254; b) Corrie, T. J. A.; Lloyd-Jones, G. C., Formal Synthesis of (±)-Allocolchicine Via Gold-Catalysed Direct Arylation: Implication of Aryl Iodine(III) Oxidant in Catalyst Deactivation Pathways. *Top. Catal.* **2017**, *60***,** 570–579; c) C. Nottingham, C.; V. Barber, V.; Lloyd-Jones, G. C. *Org. Synth.* **2019**, *96*, 150–178.

(16) Arylgermanes have recently been developed by Schoenebeck as highly reactive and functional-group tolerant alternatives to arylsilanes (references 12-15) see: a) Fricke, C.; Dahiya, A.; Reid, W. B.; Schoenebeck, F. Gold-Catalyzed C–H Functionalization with Aryl Germanes. *ACS Catalysis*, **2019,** *9*, 9231–9236. b) Fricke, C.; Sherborne, G. J.; Funes-Ardoiz, I.; Senol, E.; Guven, S.; Schoenebeck, F. Orthogonal Nanoparticle Catalysis with Organogermanes. *Angew. Chem. Int. Ed*. **2019**, *58*, 17788-17795; c) Dahiya, A.; Fricke, C.; Schoenebeck, F. Gold-Catalyzed Chemoselective Couplings of Polyfluoroarenes with Aryl Germanes and Downstream Diversification. *J. Am. Chem. Soc*. **2020**, *142*, 7754-7759; (d) Sherborne, G. J.; Gevondian. A. G.; Funes-Ardoiz. I.; Dahiya, A.; Fricke, C.; Schoenebeck, F. Modular and Selective Arylation of Aryl Germanes ($CGeEt_3$) over CBpin, CSiR3 and Halogens Enabled by Light-Activated Gold Catalysis. *Angew. Chem. Int. Ed*. **2020**, *59*, DOI 10.1002/anie.202005066; (e) Fricke, C.; Deckers, C.; Schoenebeck, F.; Orthogonal Stability & Reactivity of Aryl Germanes Enables Rapid and Selective (Multi)Halogenations. *Angew. Chem. Int. Ed*. **2020**, *59*, DOI 10.1002/anie.202008372; (f) Fricke, C.; Reid, W.; Schoenebeck, F.; A Review on Gold-Catalyzed C-H Arylation of Arenes – Challenges and Opportunities. Eur. J. Org. Chem., **2020**, DOI: 10.1002/ejoc.202000856.

(17) For reviews on the synthesis of functional organic materials *via* C–H functionalisation see: a) Kuninobu, Y.; Suekia, S. C–H Bond Transformations Leading to the Synthesis of Organic Functional Materials. *Synthesis* **2015**, *47*, 3823–3845; b) Segawa, Y.; Maekawa, T.; Itami, K. Synthesis of Extended π-Systems through C–H Activation. *Angew. Chem. Int. Ed.* **2015**, *54*, 66–81.

(18) The core arylated-fluorene motif in **4** is present in ledipasvir: Link, J. O.; Taylor, J. G.; Xu, L.; Mitchell, M.; Guo, H.; Liu, H.; Kato, D.; Kirschberg, T.; Sun, J.; Squires, N.; Parrish, J.; Keller, T.; Yang, Z.-Y.; Yang, C.; Matles, M.; Wang, Y.; Cheng, G.; Tian, Y.; Mogalian, E.; Mondou, E.; Cornpropst, M.; Perry, J.; Desai, M. C. Discovery of ledipasvir (GS-5885): a potent, once-daily oral NS5A inhibitor for the treatment of hepatitis C virus infection. *J. Med. Chem.* **2014**, *57*, 2033−2046

(19) The contraction 'intra-inter' is used in place of 'intramolecular-intermolecular' throughout this work; 'inter-intra' denote the reverse sequence

(20) For Au-catalyzed couplings of other silyl species, see for example: Kim, S.; Rojas-Martin, J.; Toste, F. D. Visible light-mediated gold-catalysed carbon(sp2)–carbon(sp) cross-coupling. *Chem. Sci*., **2016**, *7*, 85–88; b) Akram, M. O.; Mali, P. S.; Patil, N. T. Cross-Coupling Reactions of Aryldiazonium Salts with Allylsilanes under Merged Gold/Visible-Light Photoredox Catalysis. *Org. Lett*. **2017**, *19*, 3075−3078; c) Alcaide, B.; Almendros, P.; Busto, E.; Laźaro-Milla, C. Photoinduced Gold-Catalyzed Domino C(sp) Arylation/Oxyarylation of TMS-Terminated Alkynols with Arenediazonium Salts. *J. Org. Chem*. **2017**, *82*, 2177−2186; d) Hopkinson, M. N.; Tlahuext-Aca, A.; Glorius, F. Merging Visible Light Photoredox and Gold Catalysis. *Acc. Chem. Res*. **2016**, *49*, 2261−2272, and references therein.

(21) For selected reactions involving aryl-gold intermediates see: a) Chakrabarty, I.; Akram, M. O.; Biswas, S.; Patil, N. T. Visible Light Mediated Desilylative C(Sp2)–C(Sp2) Cross-Coupling Reactions of Arylsilanes with Aryldiazonium Salts Under Au(I)/Au(III) Catalysis. *Chem. Commun*. **2018**, *54*, 7223–226; b) Harper, M. J.; Arthur, C. J.; Crosby, J.; Emmett, E. J.; Falconer, R. A.; Fensham-Smith, A. J.; Gates, P. G.; Leman, T.; McGrady, J. E.; Bower, J. F.; Russell, C. A. Oxidative Addition, Transmetalation, and Reductive Elimination at a 2,2′-Bipyridyl-Ligated Gold Center. *J. Am. Chem. Soc.* **2018**, *140*, 4440–4445; c) Carrillo-Arcos, U. A.; Porcel, S. Gold Promoted Arylative Cyclization of Alkynoic Acids with Arenediazonium Salts. *Org. Biomol. Chem.* **2018**, *16*, 1837–1842; d) Akram, M. O.; Shinde, P. S.; Chintawar, C. C.; Patil, N. T. Gold(I)-Catalyzed Cross-Coupling Reactions of Aryldiazonium Salts with Organostannanes.

*Org. Biomol. Chem.* **2018**, *16*, 2865–2869; e) Rochigiani, L.; Fernandez-Cestau, J.; Budzelaar, P. H. M. Bochmann, M. Reductive Elimination Leading to C−C Bond Formation in Gold(III) Complexes: A Mechanistic and Computational Study. *Chem. Eur. J.* **2018**, *24*, 8893–8903; f) Hofer, M.; Genoux, A.; Kumar, R.; Nevado, C. Gold-Catalyzed Direct Oxidative Arylation with Boron Coupling Partners. *Angew. Chem. Int. Ed.* **2017**, *56*, 1021–1025; g) Gauchot, V.; Sutherland D. R.; Lee, A.-L. Dual Gold and Photoredox Catalysed C–H Activation of Arenes for Aryl–Aryl Cross Couplings. *Chem. Sci*, **2017**, *8*, 2885–2889; h) Rekhroukh F.; Blons C.; Estévez, L.; Mallet-Ladeira, S.; Miqueu, K.; Amgoune, A.; Bourissou. D. Gold(III)–Arene Complexes by Insertion of Olefins Into Gold–Aryl Bonds. *Chem. Sci*, **2017**, *7*, 4539–4545; i) Serra, J.; Parella, T.; Ribas. X. Au(III)-Aryl Intermediates in Oxidant-Free C–N and C–O Cross-Coupling Catalysis. *Chem. Sci*, **2017**, *7*, 946–952; j) Harper, M. J.; Emmett, E. J.; Bower, J. F.; Russell, C. A. Oxidative 1,2-Difunctionalization of Ethylene via Gold-Catalyzed Oxyarylation. *J. Am. Chem. Soc.* **2017**, *139*, 12386–12389; k) Kang, K.; Liu, S.; Xu, T.; Wang, D.; Leng, X.; Bai, R.; Lan, Y.; Shen, Q. C(sp2)–C(sp2) Reductive Elimination from Well-Defined Diarylgold(III) Complexes. *Organometallics*, **2017**, *36*, 4727–4740; l) Sauer, C.; Liu, Y.; A. De Nissi, Protti, S.; Fagnoni, M.; Bandini, M. Photocatalyst-free, Visible Light Driven, Gold Promoted Suzuki Synthesis of (Hetero)biaryls. *ChemCatChem*, **2017**, *9*, 4456–4459.

(22) To emulate the conditions of the domino sequence, 3 mol% tht.$AuBr_3$, in a solvent mixture of 100:1 $CDCl_3$/$CD_3OD$, was employed in the arylation of **1a**, using double the quantity of oxidant [$PhI(OAc)_2$] and acid (CSA) theoretically required.

(23) We use the term 'partition' to refer the ratio of two *rate constants* (i.e., $k_1/k_2$), rather than the ratio of absolute rates ($k_1$[**1**]/$k_2$[**2**]), noting that the latter quantity is subject to variation with conversion if $k_1 \neq k_2$, and possibly also to disparity of the molecularity of the steps being compared.,

(24) For example, **3c** gives *p*-F-**4c** in >99:1 *rr*, (compare, 95:5 entry 2) and *p*-F-**3e** gives *p*-F-**4e** in 88:12 *rr* (compare 60:40, entry 4). To verify the >99:1 *rr* regioselectivity, an authentic sample of *iso-p*-F-**4c** was prepared *via* an independent synthetic route. See Supporting Information for details.

(25) Electron-withdrawing arylsilane substituents reduce C–Si auration rates ($\rho = -1.6$; see reference 13).

(26) Several unidentified side reactions precluded full analysis; authentic samples of intermediates were independently prepared to confirm assignments, see SI. Biphasic-kinetics are observed in the early phases of accumulation of **3c**. This phenomenon is being investigated in detail and will be reported on in full in due course.

(27) Exceptions to this general principle of accumulation occur when two processes proceed partly or completely *intramolecularly* and intermediates are not released.[5,6k] In either case, the other steps involved in catalyst turnover ($k_{T1}$, $k_{T2}$, etc.) impact on the rate of the *overall* process, but not the kinetic hierarchy

(28) For example, some of the domino reactions studied herein proceed despite poor control of the succession in catalyst speciation between the two stages ($k_1/k_2$). This is accompanied by low selectivity in the arylation step, and this provides a bypass route for the catalyst to turnover, thereby avoiding stalling, see Figure 3B. However this bypass comes at the cost of isomeric product generation and thus reduced efficiency.

## Table of Contents Graphic